

## Coastal ecosystem engineers and their impact on sediment dynamics: Eelgrass–bivalve interactions under wave exposure

Lukas Meysick <sup>1,2,3\*</sup> Eduardo Infantes <sup>4,5</sup> Luca Rugiu <sup>5</sup> Karine Gagnon <sup>1,6</sup> Christoffer Boström <sup>1</sup>

<sup>1</sup>Environmental and Marine Biology, Åbo Akademi University, Åbo, Finland

<sup>2</sup>Helmholtz Institute for Functional Marine Biodiversity at the University of Oldenburg (HIFMB), Oldenburg, Germany

<sup>3</sup>Alfred Wegener Institute Helmholtz Centre for Polar and Marine Research, Bremerhaven, Germany

<sup>4</sup>Department of Biological and Environmental Sciences, University of Gothenburg, Kristineberg, Fiskebäckskil, Sweden

<sup>5</sup>Department of Marine Sciences, University of Gothenburg, Strömstad, Sweden

<sup>6</sup>Institute of Marine Research (IMR), His, Norway

### Abstract

Habitat forming ecosystem engineers play critical roles in structuring coastal seascapes. Many ecosystem engineers, such as seagrasses and epifaunal bivalves, are known to have positive effects on sediment stability and increase coastal protection and ecosystem resilience. Others, such as bioturbating infaunal bivalves, may instead destabilize sediment. However, despite the common co-occurrence of seagrasses and bivalves in coastal seascapes, little is known of their combined effects on sediment dynamics. Here, we used wave flumes to compare sediment dynamics in monospecific and multispecific treatments of eelgrass, *Zostera marina*, and associated bivalves (infaunal *Limecola balthica*, infaunal *Cerastoderma edule*, epifaunal *Magellana gigas*) under a range of wave exposures. Eelgrass reduced bedload erosion rates by 25–50%, with digital elevation models indicating that eelgrass affected the sediment micro-bathymetry by decreasing surface roughness and ripple sizes. Effects of bivalves on sediment mobilization were species-specific; *L. balthica* reduced erosion by 25%, *C. edule* increased erosion by 40%, while *M. gigas* had little effect. Importantly, eelgrass modified the impacts of bivalves: the destabilizing effects of *C. edule* vanished in the presence of eelgrass, while we found positive additive effects of eelgrass and *L. balthica* on sediment stabilization and potential for mutual anchoring. Such interspecific interactions are likely relevant for habitat patch emergence and resilience to extreme wave conditions. In light of future climate scenarios where increasing storm frequency and wave exposure threaten coastal ecosystems, our results add a mechanistic understanding of sediment dynamics and interactions between ecosystem engineers, with relevance for management and conservation.

In coastal soft sediments, ecosystem engineers (*sensu* Jones et al. 1994) can shape entire ecological landscapes and thereby often contribute disproportionately to ecosystem functioning and ecosystem service provisioning (Bouma et al. 2009; Gutiérrez et al. 2011). Due to the negative interactive effects of climate change, coastal development and other anthropogenic stressors, however, coastal ecosystems are among the most degraded around the globe, and the associated functions they provide are in decline (Halpern et al. 2008). Sediment erosion will likely become an additional challenge to these

ecosystems as storm intensities, sea level rise, and flooding events increase (Ranasinghe 2016; Collins et al. 2019). The intensity of destructive storms in Northern Europe, for example, has increased by more than a factor of three since 1990 (Gregow et al. 2017). The consequences of these changes for shoreline stability are unprecedented and hard to foresee (Roebeling et al. 2013; Łabuz 2015), thus stimulating a growing interest in the resilience of associated ecological communities and their role in sediment stabilization and shoreline protection (Bouma et al. 2014; Ondiviela et al. 2014).

Some ecosystem engineers, such as coastal vegetation and reef-forming bivalves, which create structurally complex biogenic habitats, function as critical sediment stabilizers (Hansen and Reidenbach 2012; Ysebaert et al. 2019). For example, seagrass canopy structure can dissipate wave energy and reduce current and oscillatory flow velocities (Fonseca et al. 1982; Hansen and Reidenbach 2012; Infantes et al. 2012). The resulting lower shear stress on the sediment surface reduces

\*Correspondence: lukas.meyssick@hifmb.de

This is an open access article under the terms of the Creative Commons Attribution License, which permits use, distribution and reproduction in any medium, provided the original work is properly cited.

Additional Supporting Information may be found in the online version of this article.

sediment resuspension and bed load erosion (Chen et al. 2007; Hansen and Reidenbach 2012; Marin-Diaz et al. 2020). Simultaneously, seagrasses affect sediment dynamics by particle trapping (Hendriks et al. 2008), sediment binding (Marin-Diaz et al. 2020), and by promoting microphytobenthos growth on the sediment surface (Widdows et al. 2008).

Similarly, bivalves such as oysters and mussels can facilitate sediment stability when forming dense patches and reefs, as their biogenic structures attenuate wave energy and reduce flow velocities (Wiberg et al. 2019; Ysebaert et al. 2019). Low-density oysters and mussel patches are less studied, but could potentially increase sediment erosion by promoting turbulent flow near the sediment bed (Meadows et al. 1998; Meysick et al. 2019a). The role of infaunal bivalves, such as clams and cockles, in sediment dynamics is likely grain size dependent (Cozzoli et al. 2020). In muddy, cohesive sediments, infaunal bivalves tend to promote erodibility and resuspension through bioturbation (Willows et al. 1998; Ciutat et al. 2007), whereas they might have a more stabilizing role in sandy sediments possibly associated with different feeding modes (Donadi et al. 2014; Cozzoli et al. 2020).

Currently, the effect of coastal ecosystem engineers on the modulation of sediment micro-bathymetry (sediment surface complexity on a millimeter to centimeter scale)—a critical parameter that drives sediment stability (Papanicolaou et al. 2001), transport and fate of organic matter including propagules (Danovaro et al. 2001; Meysick et al. 2019a) as well as the spatial organization of benthic communities (Danovaro et al. 2001; Damveld et al. 2018)—remains unknown.

Importantly, different ecosystem engineers naturally often inhabit the same environments, interact with each other and thereby may modify ecosystem processes synergistically or antagonistically (González-Ortiz et al. 2014; Passarelli et al. 2014; Angelini et al. 2015). Such concurrent modifications, however, are complex and can be difficult to predict based on individual effects as they may display nonadditivity (Passarelli et al. 2014; Donadi et al. 2015; Flynn et al. 2020). To quantify sediment dynamics in shallow coastal environments, including sediment surface bathymetry and ripple formation, it is therefore critical to investigate how co-occurring ecosystem engineers function both individually and in co-occurrence. This is especially true for seagrasses and bivalves that often live in association and interact through facultative mutualism (Fales et al. 2020; Gagnon et al. 2020), since despite their demonstrated value for hydrodynamics and sediment dynamics, combined effects of these species have yet to be reported.

The shallow coastal zones of the Baltic Sea provide a model system to bridge this knowledge gap and to examine the interactions of the dominant seagrass species, eelgrass *Zostera marina* (Boström et al. 2014) with associated bivalve species, including the often highly abundant infaunal *Limecola balthica* (Baltic clam; formerly *Macoma balthica*) and *Cerastoderma edule* (edible cockle) (Boström and Bonsdorff 1997, Herkül and Kotta 2009, Meysick et al. 2019b; Supporting Information Fig. S1), and the

introduced epifaunal *Magellana gigas* (Pacific oyster; formerly *Crassostrea gigas*), which has been found associated with eelgrass at low densities in the Skagerrak area (Infantes pers. obs.). Wave exposure is the primary driver for sediment transport in these zones because tidal oscillations are minimal in the Baltic Sea (Jönsson et al. 2005).

We performed two wave flume experiments with monospecific and multispecific treatments of eelgrass and three associated bivalves (*L. balthica*, *C. edule*, *M. gigas*) at natural densities found in the northern Baltic Sea and the Skagerrak. Our main aims were to (1) assess how eelgrass and bivalves physically interact with each other under wave exposure; (2) quantify how these ecosystem engineers affect sediment erosion rates and micro-bathymetry relative to bare sediments; and (3) assess whether and under which conditions they affect sediment dynamics synergistically or antagonistically (Fig. 1).

## Materials and Methods

### Eelgrass and *L. balthica*: Sediment stability, interactions, and behavior (Experiment 1)

In Experiment 1, we investigated the interactions of eelgrass and *L. balthica* and their effects on sediment stability under a range of wave exposures, using a semi-outdoor wave mesocosm facility at the Archipelago Centre Korpoström, Finland between July and September 2018.

In the region near the island of Fårö (59°55'N, 21°47'E) in the outer Finnish Archipelago Sea, *L. balthica* (> 5 mm) occurs in high densities (~2000 ind. m<sup>-2</sup>) in eelgrass meadows (Meysick et al. 2020). Here, we collected *L. balthica*, eelgrass shoots and sediment for the experiment. We stored bivalves (regularly fed with detritus) and plants separately in flow-through seawater aquaria with filtered water pumped from the nearby harbor (3 m depth). We sieved sediment using a 0.8 mm mesh and air-dried it prior the experiment to remove any remaining macrofauna. We then determined sediment grain size distribution by dry sieving methods: the dominant grain size class was fine sand (125–250 μm, 88.2%), silt content was < 0.1%, and median grain size ( $D_{50}$ ) was 184 μm (Supporting Information Fig. S3). Sediment organic content at the field site is overall low (0.35%; Meysick et al. 2020).

We used four identical hydraulic wave mesocosms of 3 m length, 0.5 m width, and 0.8 m height (for detailed description, see Infantes et al. 2021). Waves were generated with a moving paddle driven by a pneumatic piston. To dissipate waves and to reduce reflection, a wave dampener (4 : 5 slope) made of porous plastic fiber was placed at the end of the tank. Each mesocosm included a 20-cm deep double bottom, in which a 50 × 50 × 10 cm (length × width × height) box (test section) was embedded in the center.

We investigated sediment erosion rates in a factorial combination of eelgrass and *L. balthica* fully crossed with four wave exposure treatments. Each of the wave tanks was calibrated to

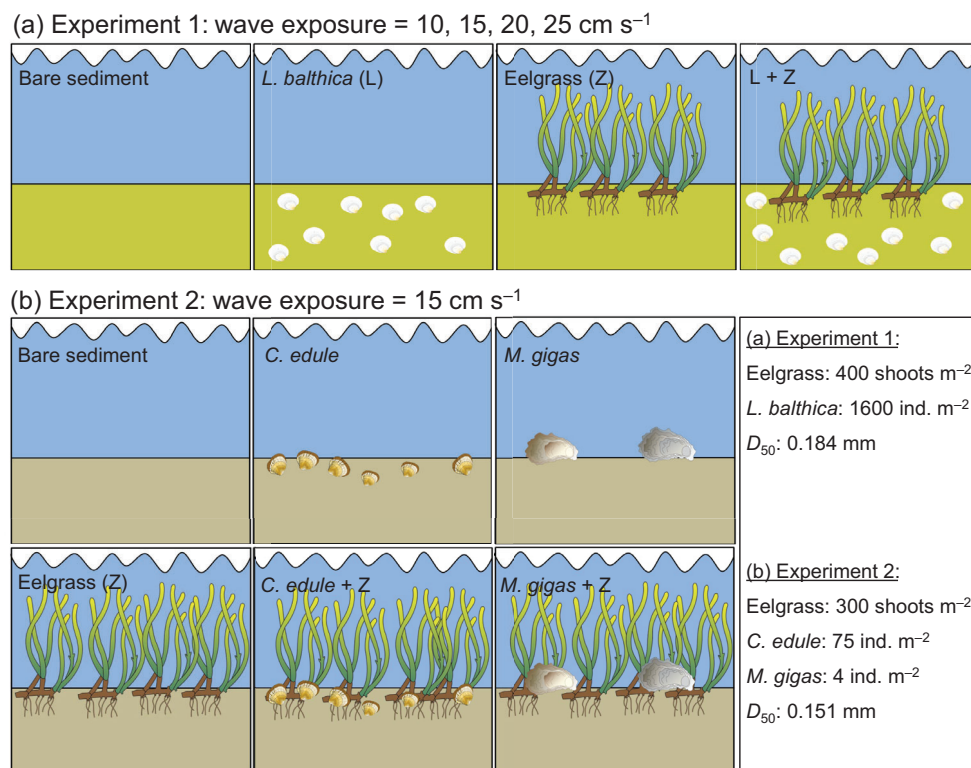


**Fig. 1.** Investigated species treatments in wave flumes to quantify (a) sediment erosion and species interactions at different wave exposures, and (b) sediment erosion and micro-bathymetry through sediment roughness parameters. Images (seagrass, oysters) from IAN Symbol Libraries. Photographs of the respective wave mesocosms can be found in Supporting Information Fig. S2.

a set wave regime (approximate mean orbital velocities [ $U_{rms}$ ] = 10, 15, 20, and 25 cm s<sup>-1</sup> with a constant wave period [ $T_p$ ] of ~3.6 s), simulating a hydrodynamic gradient with maximum bottom shear velocities ( $U_*$ ) between 1 and 3 cm s<sup>-1</sup>. These shear velocities represent moderate to severe storm events in Baltic Sea shallow coastal areas with short fetch (Jönsson et al. 2005; Infantes et al. 2021). Individual treatments were replicated three times, resulting in 48 trials in total. Prior to each trial, we sealed gaps between the double bottom and the wave tank wall with aluminum tape to avoid sediment loss. We added sediment to the test section and leveled it to the height of the double bottom, then filled the tanks with seawater from the harbor (salinity: 6) to a water level of 25 cm. In eelgrass treatments, we planted 100 eelgrass shoots randomly within the test section, by carefully pushing the rhizomes  $\leq 5$  cm below the sediment surface. In *L. balthica* treatments, we evenly spread ~400 clams on top of the sediment. After several hours, we replaced individuals still on the surface, until approximately 95% of *L. balthica* had burrowed into the sediment. Remaining individuals were removed before starting the experiments. We trimmed eelgrass shoots before being used to assure similar leaf and rhizome lengths (20 and 8 cm, respectively). Average *L. balthica* size used for this experiment was  $11.0 \pm 0.3$  mm (SE,  $n = 15$ ). Density of eelgrass shoots and *L. balthica* corresponded to 400 and

1600 m<sup>-2</sup>, respectively, representing typical densities found in the Finnish Archipelago Sea (Meysick et al. 2020).

Sediment was allowed to compact for 24 h, followed by 1 h of wave exposure. After termination and sufficient time for resuspended sediment to settle (~30 min), we carefully collected all sediment that had moved beyond the test section (both downstream and upstream) using a suction hose. We then oven-dried the sediment at 100°C until constant weight (~48 h) and weighed it to determine the sediment erosion rate of the test section (g m<sup>-2</sup> h<sup>-1</sup>) for each trial. We counted the number of eelgrass shoots and *L. balthica* that had been dislodged during wave exposure. To determine *L. balthica* behavior in the form of vertical migration, we took five 10-cm deep sediment cores (diameter,  $\varnothing = 5$  cm) from each *L. balthica* trial. We sliced the cores into four sections (0–2, 2–4, 4–6, and 6–10 cm depth intervals) and counted the number of *L. balthica* per section.

#### Eelgrass, *C. edule*, and *M. gigas*: Sediment stability and surface complexity (Experiment 2)

In Experiment 2, we investigated the interactions of eelgrass with the two bivalves *M. gigas* and *C. edule*, and their effects on sediment erosion and bathymetry at Kristineberg Marine Research Station, Sweden, between August and September 2018. We collected eelgrass shoots, bivalves, and

sediment at Bökevik in the Gullmars Fjord, Sweden (58°25'N, 11°45'E). When not in use, we stored animals and plants in tanks with flow-through seawater from the fjord (5 m depth). We sieved the sediment beforehand using a 2-mm mesh. We then determined sediment grain size distribution by dry sieving methods and sediment organic content by loss-on-ignition. Dominant grain size class was fine sand (125–250  $\mu\text{m}$ , 63.4%),  $D_{50}$  was 151  $\mu\text{m}$ , silt content (< 63  $\mu\text{m}$ ) was 1.2% (Supporting Information Fig. S3), and sediment organic content was 0.55%.

We used a hydraulic wave flume of 8 m length, 0.5 m width, and 0.5 m height. The wave generating system resembles the one from the mesocosms in Experiment 1. To dissipate wave energy, a wave dampener (1:5 slope) made of porous artificial fiber and reinforced with a PVC layer was placed at the end of the tank. The test section was composed of a 200  $\times$  37  $\times$  20 cm embedded box (length  $\times$  width  $\times$  height). We filled the box with sediment and carefully leveled it to the height of the flume bottom surface (20 cm sediment depth). We then filled the flume with seawater from the fjord (water level: 25 cm, salinity: 34).

In eelgrass treatments, we randomly planted 200 shoots within the test section (see Experiment 1). The resulting shoot density of 300 shoots  $\text{m}^{-2}$  corresponds to densities typically found in the region (Boström et al. 2014). In *C. edule* treatments, we evenly distributed 80 cockles across the test section. We replaced all cockles that had not burrowed in the sediment after 1 h until on average  $56 \pm 4.1$  cockles burrowed in the sediment ( $\sim 75$  ind.  $\text{m}^{-2}$ ). This represents an environmentally realistic intermediate density of *C. edule* found in soft sediments of the Baltic Sea-Skagerrak region ( $\sim 5$ –200 ind.  $\text{m}^{-2}$ , Lindegarth et al. 1995, Obolowski et al. 2007), also found associated with eelgrass (Herkül and Kotta 2009). *M. gigas*, on the

other hand, rarely exceeds densities of 5 ind.  $\text{m}^{-2}$  when intermixed with eelgrass in this area (Infantes pers. obs.). To reflect natural intermixed conditions, we added three oysters in *M. gigas* treatments, corresponding to 4 ind.  $\text{m}^{-2}$  (Fig. 2b). To achieve a maximal effect on sediment dynamics, we oriented the oysters offset across the width of the flume (the flat part facing the bottom). We trimmed eelgrass shoots to 20 cm leaf length and 8 cm rhizome length. Average size of *M. gigas* and *C. edule* was  $117.7 \pm 2.2$  mm (SE,  $n = 3$ ) and  $28.7 \pm 0.8$  mm (SE,  $n = 10$ ), respectively.

We applied an intermediate wave exposure treatment with  $U_{\text{rms}}$  of approximately  $15 \text{ cm s}^{-1}$  for 1 h. As sediment was not fully removed between treatments, we reduced sediment compaction time to 2 h. After each trial was terminated, the sediment was given 30 min to resettle. We then slowly ( $\sim 20$  min) drained the water from the flume to minimize disturbance of the sediment surface and to allow for the construction of high-quality digital elevation models (DEMs) (see below). We collected all sediment that had moved beyond the test section using a suction hose. In eelgrass treatments, we carefully cut shoots at the sediment surface with scissors so that the shoots floated to the water surface and could be collected without disturbing the sediment. We used a pneumatic pump system to drain remaining water from between the sand ripples. Subsequently, we marked the edges of the test section with measuring tape as reference and took 100–150 images of the sediment surface from different angles for generating DEMs.

### Sediment micro-bathymetry

To quantify the effects of eelgrass and bivalves on sediment micro-bathymetry after wave exposure, we built DEMs using the software Agisoft® PhotoScan Professional v1.4.4. First,

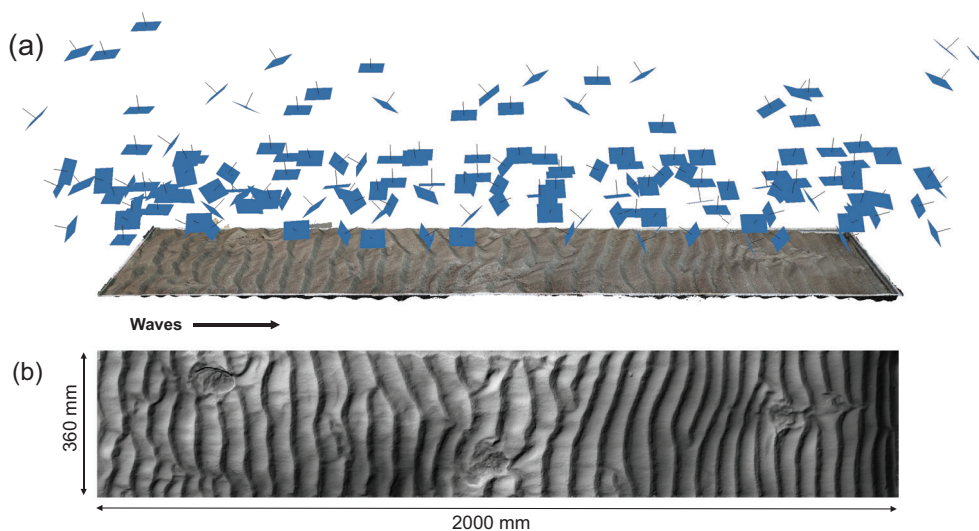


**Fig. 2.** Photogrammetry analysis in Experiment 2. Example of (a) sediment bathymetry model with the corresponding camera positions of the images (blue rectangles,  $n = 100$ –150) and (b) the resulting DEM (treatment: unvegetated sediment with oysters).

sediment surface images were loaded to the program and aligned in a triangulation process (see Leon et al. 2015), generating a sparse point cloud of the test section. We then assembled the sparse point cloud with 30 evenly distributed marker points, based on measuring tape and benchmarks within the test section. If necessary, we corrected marker points manually in each image of appearance. We assigned three-dimensional coordinates (length:  $x$ , width:  $y$ , height:  $z$ ; in mm) to each point to create a local coordinate system of the test section. The point cloud was optimized by deleting points according to reconstruction uncertainty ( $> 10$ ), reprojection error ( $> 0.5$ ), and projection accuracy ( $> 15$ ), using the in-built “gradual selection” function, and by manually deleting outliers. We then optimized camera alignment through adaptive camera model fitting based on marker points and the optimized point cloud. After constructing a low-quality mesh within the region of interest, we masked the model accordingly and constructed a dense point cloud. Methodology for deriving high-quality dense point clouds roughly followed Mallison and Wings (2014). After removal of obvious outliers, we built the DEMs based on the dense point cloud. To reduce friction and boundary effects along the edges at the sediment box, the DEMs were embedded with 0.5 cm distance from all edges. Parameterizations for all steps can be found in Supporting Information Table S1. An example for an image alignment, the corresponding dense point cloud, and a DEM is given by Fig. 2.

We loaded individual DEMs to Matlab v.R2019b and, to match pixel resolution for all treatments, interpolated the models to highest common resolution possible using the “griddedInterpolant” function. We approximated sediment complexity using several sediment roughness parameters. The root mean square (RMS) height ( $\xi$ ) is the standard deviation of the vertical elevation and thus describes the overall deviation from a flat surface. It is a common measure for surface heterogeneity and is calculated as

$$\xi = \sqrt{\frac{1}{n} \sum_{i=1}^n (z_i - \bar{z})^2}, \quad (1)$$

where  $z_i$  is the height at location  $i$  ( $x, y$  coordinate), and  $\bar{z}$  is the mean height of the sediment surface (Shepard et al. 2001). The RMS slope ( $\theta_{\text{rms}}$ ) is the root mean square slope between points  $z(x_i)$  and  $z(x_i + \Delta x)$ , which are separated by the step size  $\Delta x$  (Shepard et al. 2001). We used  $\Delta x = 0.059$  mm, which corresponds to the pixel resolution after interpolation. The RMS slope is given by

$$\theta_{\text{rms}} = \tan^{-1} \left( \frac{v(\Delta x)}{\Delta x} \right), \quad \text{with } v = \sqrt{\frac{1}{n} \sum_i (z(x_i) - z(x_i + \Delta x))^2}. \quad (2)$$

Rugosity,  $f_r$  (or tortuosity index), describes the augmentation of the sediment surface compared to a flat surface and thus can take on values equal to or greater than 1.

Rugosity was calculated as

$$f_r = \frac{A_r}{A_g}, \quad (3)$$

where  $A_r$  is the true (3D) surface area of the sediment surface and  $A_g$  is the geometric (2D) surface area of the sediment surface. The true surface area was derived from the “demarea” function, which uses triangulation of each cell with its eight neighboring cells (Duge 2022).

To determine mean ripple height,  $h$ , and ripple length,  $l$ , we additionally interpolated the DEM to a lower resolution of 0.33 mm/pix to exclude local deviations in between ripples. Based on 15 transects (in direction of wave propagation), we determined the number of ripples and individual ripple heights by the “findpeaks” function in Matlab. Ripple height was then averaged across all transects. Ripple length was determined by the number of ripples per transect divided by the total transect length, averaged across all 15 transects. Maximum elevation,  $h_{\text{max}}$ , per trial was determined by the difference between maximal crest and maximal trough height within the test section.

### Flow measurements

For both experiments, we measured orbital flow velocities for each trial using an Acoustic Doppler Velocimeter (Nortek, Vectrino), at a sampling rate of 25 Hz for 3 min. In Experiment 1, we measured vertical profiles (1–16 cm above sediment) in the center of the test section. In Experiment 2, we measured vertical profiles (1–13 cm above sediment) 60 cm upstream, in the center, and 60 cm downstream of the test section. We then calculated mean orbital velocities ( $U_{\text{rms}}$ ) for each position as follows:

$$U_{\text{rms}} = \sqrt{\frac{1}{N} \sum_{i=1}^n (u_i^2)}, \quad (4)$$

where  $n$  is the number of measurements ( $n = 4500$ ) and  $u$  is the horizontal component of the orbital velocity, directional to the wave propagation. In Experiment 1,  $U_{\text{rms}}$  at unobstructed flow (i.e., without eelgrass canopy) corresponded to  $11.8 \pm 0.8$ ,  $14.7 \pm 0.2$ ,  $20.7 \pm 0.5$  and  $23.7 \pm 0.1$   $\text{cm s}^{-1}$  (mean  $\pm$  SE). In Experiment 2,  $U_{\text{rms}}$  was  $15.2 \pm 0.1$   $\text{cm s}^{-1}$ . To compare near bottom hydrodynamic forces for each set wave treatment with realistic field conditions (Jönsson et al. 2005), we calculated bottom shear velocities  $U_*$  as:

$$U_* = U_0 \sqrt{0.5 f_w},$$

where  $U_0$  is the maximum orbital velocity above bottom boundary layer and  $f_w$  is the wave friction factor which can be calculated based on the grain size ( $D_{50}$ ) as:



$$f_w = \exp\left(5.5 \left(\frac{A_b}{2.5 D_{50}}\right)^{-2} - 6.3\right),$$

where  $A_b$  is the maximum orbital amplitude. Values for  $U_*$  represented a range of annual maximum shear velocities found in shallow areas across the Baltic Sea (Experiment 1:  $1.38 \pm 0.11$ ,  $1.60 \pm 0.10$ ,  $2.22 \pm 0.13$ ,  $2.56 \pm 0.06$ , Experiment 2:  $1.65 \pm 0.11$ ; Jönsson et al. 2005). Wave conditions and vertical profiles of flow velocity for each experiment can be found in Supporting Information Figs. S4–S7 and Table S2.

### Statistical analysis

In Experiment 1, we first used a two-way general linear model (LM) to analyze the effects of eelgrass presence (with or without) and wave exposure ( $U_{\text{rms}} = 10\text{--}25 \text{ cm s}^{-1}$ ) on bottom shear velocities ( $U_*$ ). We then assessed whether eelgrass and *L. balthica* presence as well as wave exposure affected sediment erosion using a three-way LM. We further used two-way generalized linear models (GLM) to analyze the effects of *L. balthica* presence on eelgrass shoot dislodgement and vice versa with wave exposure as covariate. We chose a Poisson error distribution to account for heterogeneous variance. Finally, we analyzed *L. balthica* vertical distribution using a three-way generalized linear mixed model (GLMM) with sediment depth (4 cm depth intervals) and eelgrass presence as factors and wave exposure as covariate. Replicate corer was included as a random factor, as five (pseudo-)replicates were taken per trial. A Poisson error distribution was used to account for heterogeneous variance.

In Experiment 2, we first used one-way ANOVA to analyze the effect of eelgrass presence on bottom shear velocity. To

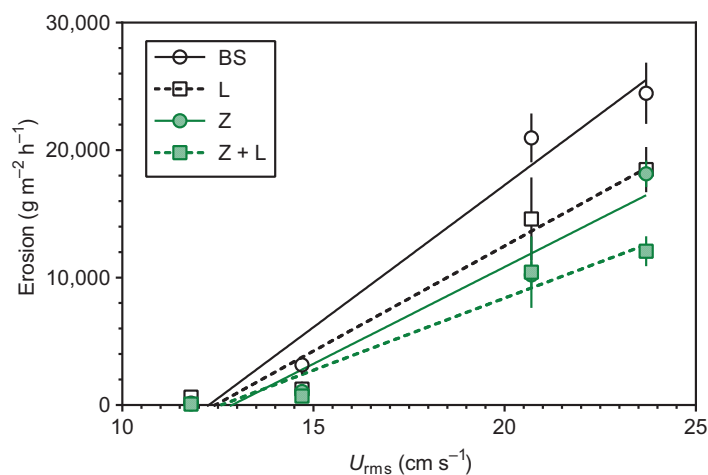


**Fig. 3.** Effect of wave exposure ( $U_{\text{rms}}$ ) on sediment erosion rates in bare sediment (BS), *Limecola balthica* (L), eelgrass (Z) and eelgrass + *L. balthica* (Z+L) treatments in Experiment 1. Values are means  $\pm$  SE ( $n = 3$ ). Lines correspond to coefficients from a three-way general linear model. [Correction added on 23 February 2022, after first online publication: The figure 3 has been replaced with the revised version]

analyze the effect of bivalve (*C. edule*, *M. gigas*) and eelgrass presence and potential interactions on sediment parameters (total erosion, RMS height, RMS slope, rugosity, ripple height, maximal height, ripple length, mean level), we used two-way ANOVAs.

For both experiments, assumptions of normality and homoscedasticity were tested by Shapiro–Wilk test and visual assessment of Q–Q and residual plots. If assumptions were not met, raw data were appropriately transformed (log, ANOVAs) or error distributions were adjusted (Poisson distribution for all GLMs and the GLMM). All data analyses were conducted in the R-environment version 3.4.0 (R Core Team 2017).

## Results

### Eelgrass and *L. balthica*: Sediment stability, interactions, and behavior

In Experiment 1, across all wave exposures, bottom shear velocity was significantly lower ( $\sim 8.5\%$ ) when eelgrass was present compared to unvegetated treatments ( $F_{1,44} = 9.66$ ,  $p = 0.003$ ; Supporting Information Table S3). The strongest reduction (21.5%) was found at  $U_{\text{rms}}$  of  $10 \text{ cm s}^{-1}$ , while at  $25 \text{ cm s}^{-1}$ ,  $U_*$  was only 3% lower in eelgrass compared to unvegetated treatments.

Overall, we found a strong positive effect of wave exposure on sediment mobilization ( $F_{1,40} = 158.52$ ,  $p < 0.001$ ; Supporting Information Table S4). In bare sediments, erosion rates increased with  $U_{\text{rms}}$  from  $150 \text{ g m}^{-2} \text{ h}^{-1}$  at  $10 \text{ cm s}^{-1}$  to almost  $25 \text{ kg m}^{-2} \text{ h}^{-1}$  at  $25 \text{ cm s}^{-1}$  (Fig. 3). This effect, however, was modulated by the presence of eelgrass ( $F_{1,40} = 8.07$ ,  $p = 0.007$ ) and *L. balthica* ( $F_{1,40} = 5.40$ ,  $p = 0.025$ ). Eelgrass reduced erosion rates by 40–55% at low and intermediate wave exposure ( $10\text{--}20 \text{ cm s}^{-1}$ ) and 25% at highest wave exposure ( $25 \text{ cm s}^{-1}$ ). *L. balthica* increased erosion by 400% at lowest wave exposure ( $10 \text{ cm s}^{-1}$ ), but reduced erosion rates by 25–60% at higher orbital velocities ( $15\text{--}25 \text{ cm s}^{-1}$ ). Interestingly, eelgrass and *L. balthica* had a positive additive effect on sediment stabilization (indicated by nonsignificant interaction,  $F_{1,40} = 0.30$ ,  $p = 0.585$ ). Hence, their combination resulted in the lowest sediment erosion rates across all exposure treatments with a 50% reduction even at highest wave exposure of  $25 \text{ cm s}^{-1}$ .

Eelgrass shoot dislodgement frequency increased significantly with wave exposure ( $\chi^2 = 442.97$ ,  $p < 0.001$ ; Supporting Information Table S5) and was overall lower (20–65%) in treatments including *L. balthica* compared to bare sediment ( $\chi^2 = 4.30$ ,  $p = 0.038$ ), except at  $U_{\text{rms}} = 15 \text{ cm s}^{-1}$  (100% higher, Fig. 4a). Similarly, *L. balthica* dislodgement increased significantly with wave exposure ( $\chi^2 = 64.93$ ,  $p < 0.001$ ; Supporting Information Table S5). Although the presence of eelgrass shoots reduced *L. balthica* dislodgement ( $\chi^2 = 11.67$ ,  $p < 0.001$ ), this was only evident at low ( $10\text{--}15 \text{ cm s}^{-1}$ : 40–90% reduction), not high ( $20\text{--}25 \text{ cm s}^{-1}$ : 0–5% increase) wave exposure ( $U_{\text{rms}} \times \text{Eelgrass}$ ,  $\chi^2 = 10.13$ ,  $p = 0.001$ , Fig. 4b).

Overall, *L. balthica* depth distribution within the sediment did not differ across all treatments ( $\chi^2 = 1.72$ ,  $p = 0.190$ ; Supporting Information Table S5). However, there was a significant Depth  $\times$  Eelgrass ( $\chi^2 = 4.24$ ,  $p = 0.039$ ) and depth  $\times$

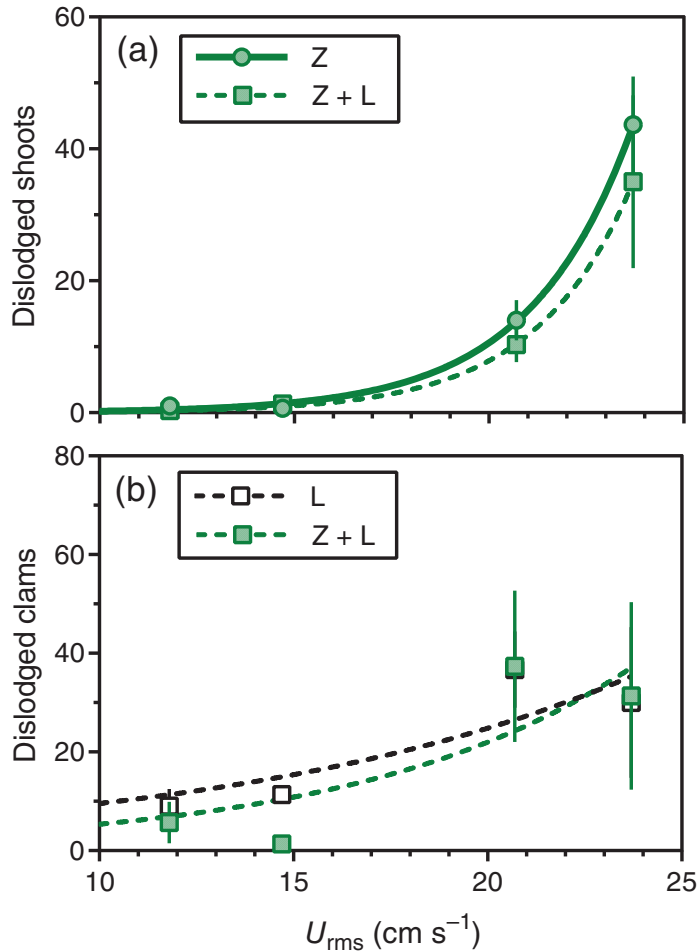


**Fig. 4.** Effect of wave exposure,  $U_{rms}$ , and (a) *Limecola balthica* (L) on eelgrass shoot dislodgement, and (b) eelgrass (Z) on *L. balthica* dislodgement. Values are means  $\pm$  SE ( $n = 3$ ). Lines correspond to coefficients from a general linear model.

$U_{rms}$  interaction ( $\chi^2 = 6.14$ ,  $p = 0.013$ ), indicating that *L. balthica* migrates vertically to deeper depths when exposure increases, and that this effect is more pronounced in unvegetated than vegetated treatments. Without eelgrass, only  $\sim 5\%$  of *L. balthica* remained in the top layer (0–2 cm) at  $U_{rms} = 25 \text{ cm s}^{-1}$  and almost 40% were found in the deepest sediment layer ( $>6 \text{ cm}$ ). In eelgrass treatments, however,  $\sim 15\%$  of *L. balthica* still remained in the top layer, while only 20% were found in the deepest layer (Fig. 5).

**Eelgrass, *C. edule*, and *M. gigas*: Sediment stability and surface complexity**

In contrast to Experiment 1, there was no effect of eelgrass canopy on bottom shear velocities ( $F_{1,16} = 0.11$ ,  $p = 0.749$ ; Supporting Information Table S6). However, there were significant effects of eelgrass ( $F_{1,12} = 157.4$ ,  $p < 0.001$ ; Supporting Information Table S6), bivalves ( $F_{2,12} = 15.26$ ,  $p > 0.001$ ), as well as a Bivalve  $\times$  Eelgrass interaction effect ( $F_{2,12} = 9.074$ ,  $p = 0.004$ ) on bedload erosion rates (Fig. 6). Without eelgrass,

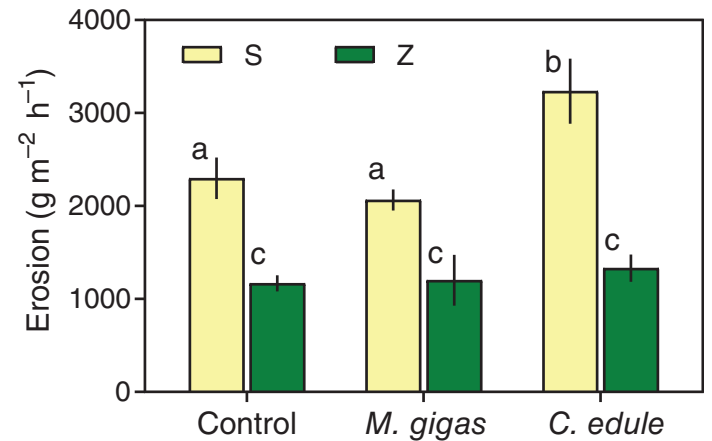


**Fig. 6.** Sediment erosion rates with bivalves (*Magellana gigas*, *Cerastoderma edule*) and without bivalves (control) in unvegetated sediment (S) and in eelgrass (Z) after 60-min wave exposure ( $U_{rms} = 15 \text{ cm s}^{-1}$ ) in Experiment 2. Different letters indicate statistical significance by  $p < 0.05$  based on Tukey HSD multiple comparison test. Values are means  $\pm$  SD ( $n = 3$ ).

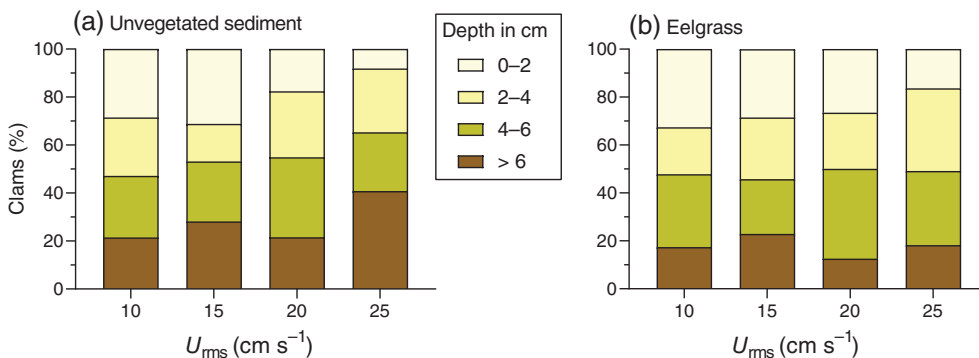


**Fig. 5.** Depth distribution of *Limecola balthica* in Experiment 1 after exposure to different wave intensities in (a) unvegetated sediment and (b) eelgrass treatments ( $n = 5$ ).

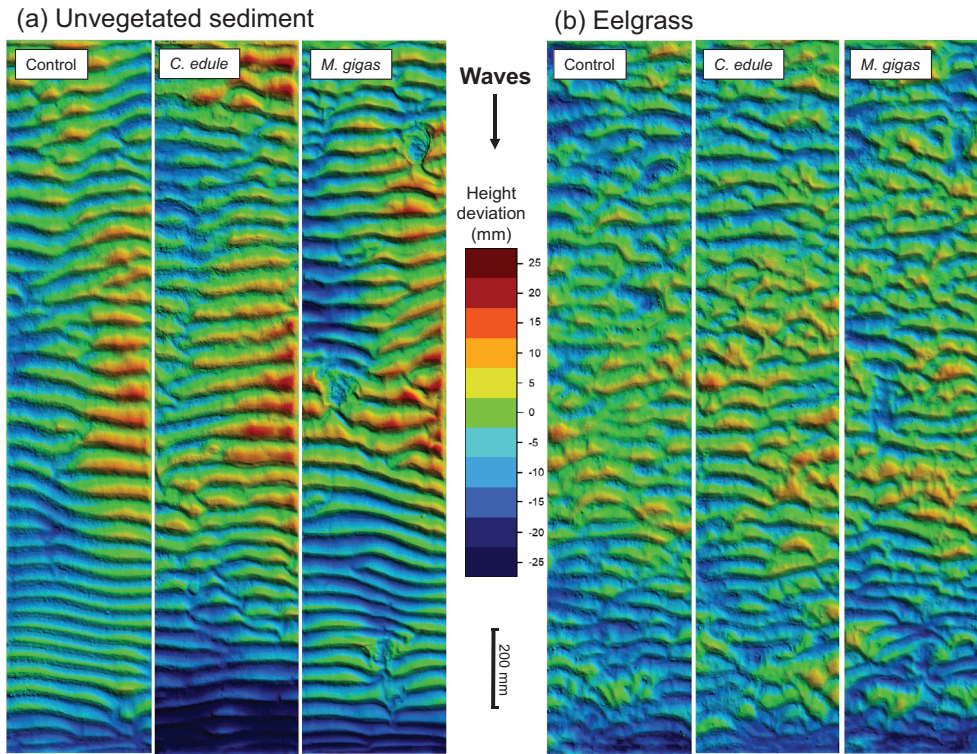


**Fig. 7.** Digital elevation models of the sediment bed characterizing surface bathymetry after 1 h wave exposure ( $U_{rms} = 15 \text{ cm s}^{-1}$ ) in control, *Cerastoderma edule* and *Magellana gigas* treatments: **(a)** in unvegetated sediment and **(b)** in eelgrass.

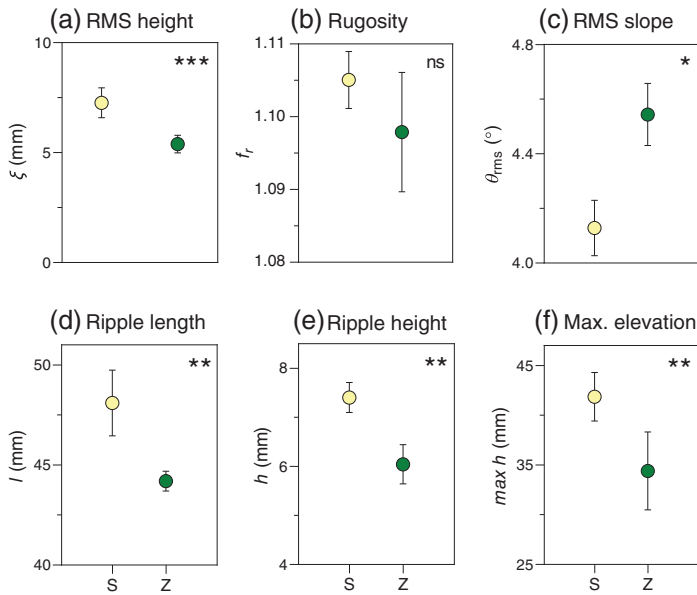


**Fig. 8.** Sediment parameters across treatments in unvegetated sediment (S, yellow) and in eelgrass (Z, green) after 1-h wave exposure ( $U_{rms} = 15 \text{ cm s}^{-1}$ ). Values are means  $\pm$  SD ( $n = 9$ ). Asterisks indicate statistically significant differences ( $*p < 0.05$ ,  $**p < 0.01$ ,  $***p < 0.001$ ) between eelgrass and unvegetated treatments based on two-way ANOVA (the main effect of bivalves was not significant for any parameter; for better visualization, y-axis does not intersect x-axis in origin for panels **b-f**).

erosion was about 40% higher in *C. edule* treatments compared to control and *M. gigas* treatments. The presence of eelgrass, however, significantly reduced erosion in all treatments to about 50% of no-bivalve treatment levels, independent of bivalve presence. Erosion rates in eelgrass and unvegetated treatments, respectively, were consistent with erosion rates from Experiment 1 at similar wave orbital velocity ( $15 \text{ cm s}^{-1}$ ). No shoots were dislodged during trials in Experiment 2.

Visual observation of the DEMs further indicated strong differences in sediment patterns between unvegetated and eelgrass treatments (Fig. 7). Sand ripples were comparably uniform in the absence of eelgrass shoots, with similar shapes in control and bivalve treatments (Fig. 7a). When eelgrass shoots were present, however, sand ripples showed non-uniform patterns, independent of bivalve presence (Fig. 7b). Analysis of sediment parameters confirmed these visual findings with overall higher sediment surface heterogeneity in unvegetated treatments (Supporting Information Table S6). While both bivalve species had no effect on sediment parameters at the investigated densities, there were significant differences between eelgrass and unvegetated treatments for most parameters, demonstrating a stabilizing effect of eelgrass (Fig. 8). The roughness parameter RMS height  $\xi$  (26% reduction,  $F_{1,12} = 27.06$ ,  $p < 0.001$ ), as well as ripple length  $l$  (9% reduction,  $F_{1,12} = 13.35$ ,  $p = 0.003$ ), ripple



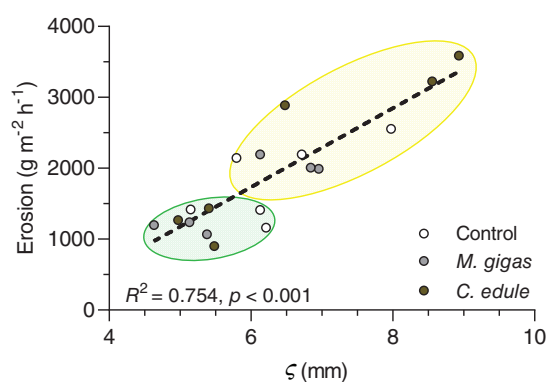


**Fig. 9.** Correlation between roughness parameter RMS height ( $\xi$ ) and sediment erosion across all treatments (control, *Magellana gigas*, *Cerastoderma edule*) in Experiment 2 ( $n = 18$ ). Yellow oval indicates treatments in unvegetated sediment, green oval indicates treatments in eelgrass.

height  $h$  (19% reduction,  $F_{1,12} = 16.83$ ,  $p = 0.001$ ), and maximal sediment elevation  $h_{\max}$  (18% reduction,  $F_{1,12} = 17.22$ ,  $p = 0.001$ ) were all significantly lower in eelgrass than in unvegetated treatments. RMS slope  $\theta_{\text{rms}}$  on the other hand was significantly higher in eelgrass treatments (10% increase,  $F_{1,12} = 5.40$ ,  $p = 0.039$ ). There was no difference in rugosity  $f_r$  between treatments ( $F_{1,12} = 0.75$ ,  $p = 0.404$ ). Independent of treatment, wave exposure ( $U_{\text{rms}} = 15 \text{ cm s}^{-1}$ ) and the associated ripple formation led to an overall sediment surface enlargement of  $\sim 15\%$  ( $f_r = 1.15$ ). Across treatments, sediment erosion and RMS height  $\xi$  were strongly correlated ( $R^2 = 0.75$ ,  $p < 0.001$ , Fig. 9).

## Discussion

We examined the role of coastal ecosystem engineers for sediment dynamics under wave exposure in single and pairwise treatments. Our results highlight that eelgrass can strongly promote sediment stabilization by reducing bottom shear velocities, erosion rates, and sediment surface roughness, while co-occurring bivalves could have either synergistic or antagonistic species-specific effects.

### Effects of eelgrass on sediment stability and micro-bathymetry

Consistent with previous studies (Chen et al. 2007; Marin-Diaz et al. 2020), we show that even small eelgrass patches at low densities (300–400 shoots  $\text{m}^{-2}$ ) can significantly stabilize sediment. Here we highlight several potential important mechanisms driving our results. In Experiment 1, eelgrass likely decreased bedload erosion rates by reducing near-bottom velocities, as earlier demonstrated for sediment resuspension (Hansen and Reidenbach 2012). Relative sediment stabilization of eelgrass was highest at wave orbital velocities between 15 and 20  $\text{cm s}^{-1}$ , where the canopy caused the highest reduction in shear velocities. In contrast, eelgrass canopy had no

effect on bottom shear velocities in Experiment 2. This might be partly related to lower shoot densities (300  $\text{m}^{-2}$  vs. 400  $\text{m}^{-2}$ ), but is more likely due to the lower wave periods used in this experiment (1.9 s vs. 3.7 s), which can reduce the canopy effect on waves (Luhar et al. 2017; Garzon et al. 2019). It is therefore likely that seagrass has contributed to sediment stability through other mechanisms such as sediment binding by rhizomes and roots (Marin-Diaz et al. 2020), and particle trapping by leaves (Hendriks et al. 2008). In Experiment 2, we also found that surface complexity (RMS height, sand ripple size, maximum bed elevation) was significantly lower in eelgrass than unvegetated sediment, and also highly correlated with bedload erosion. As sediment bathymetry strongly affects near-bed turbulence and sediment erodibility (Papanicolaou et al. 2001), this suggests that stabilization of the sediment bathymetry under wave exposure might be an important but under-regarded mechanism through which seagrass structure promotes sediment immobilization. Ecosystem processes linked to sediment bathymetry, such as sediment oxygenation (Ziebis et al. 1996), organic matter accumulation (Danovaro et al. 2001), propagule transport (Meysick et al. 2019a), and the spatial structure of associated communities (Danovaro et al. 2001; Damveld et al. 2018), might also be directly affected by this mechanism.

### Effects of bivalves on sediment stability

Both *L. balthica* and *C. edule* can promote sediment resuspension and net erosion through bioturbation, especially in intertidal areas with cohesive sediments (Willows et al. 1998; Ciutat et al. 2007). In sandy sediments where sediment transport occurs primarily as bedload, we found that *L. balthica* reduced sediment erosion rates for wave orbital velocities  $\geq 15 \text{ cm s}^{-1}$  (which corresponded to bottom shear velocities of  $\geq 1.6 \text{ cm s}^{-1}$ ). We assume that for these velocities the stabilizing effect (by providing structural complexity in form of shells and siphons) proportionally predominated the destabilizing effect through bioturbation. Indeed, previous studies indicate density, grain size, and flow dependent effects of bioturbating bivalves on sediment transport with a more stabilizing role in coarser sediment and at higher flow (Donadi et al. 2014; Cozzoli et al. 2020). Since the experimental conditions represent near-bottom hydrodynamics during moderate to severe storms in shallow Baltic Sea areas (Jönsson et al. 2005), *L. balthica* may have a previously underappreciated role for coastal stabilization due to its wide distribution at high densities in the area (Boström and Bonsdorff 1997; Meysick et al. 2020).

On the other hand, *C. edule* increased sediment erosion under wave exposure. This can in part be explained by an 18 times higher silt content (1.2%) of the sediment used in this experiment, making it more prone to bioturbation by *C. edule* (Cozzoli et al. 2020). In addition, differences in the environmental position of the bivalve species may have also played a role: cockles were partly exposed out of sediment due

to wave exposure and likely promoted turbulent flow (Ciutat et al. 2007).

Epifaunal oyster and mussel reefs are known to contribute to sediment stabilization and coastal protection (Ysebaert et al. 2019), but these effects are density dependent and decrease at lower coverage (de Paiva et al. 2018). Here, we simulated low-density oyster patches ( $< 5 \text{ ind. m}^{-2}$ ), naturally found within and near eelgrass meadows in the Skagerrak, and found that at these densities *M. gigas* has only limited effects on sediment dynamics. However, individual oysters may affect sediment heterogeneity at a small scale by locally promoting turbulent flow (Meadows et al. 1998; Meysick et al. 2019a), as indicated by elevation models (see Fig. 7), but these were not captured in net bathymetry parameters across the whole test section.

#### Co-occurring ecosystem engineers: Species interactions and effects on sediment stability

We found further that co-occurring eelgrass and *L. balthica* synergistically stabilized the sediment and in co-occurrence nearly halved sediment loss even under the highest wave regime ( $25 \text{ cm s}^{-1}$ ). Although the overall effect was small, our results also indicated mutually positive interactions through anchoring, which, in combination with sediment stabilization, might be an important mechanism for habitat patch emergence and resilience to physical disturbance. Similar facilitative effects between co-occurring ecosystem engineers have, for example, been found for cordgrass and ribbed mussels (Angelini et al. 2016), mangrove species (Huxham et al. 2010), and eelgrass and blue mussels (Reusch and Chapman 1995). Interestingly, our results also indicated that eelgrass affected *L. balthica* behavior by mitigating overall hydrodynamic conditions, because with increasing exposure clams migrated to deeper sediments depths for disturbance avoidance in unvegetated but not in vegetated treatments.

Moreover, we found antagonistic, nonadditive effects between eelgrass and *C. edule*, as eelgrass sustained low erosion rates even in the presence of this sediment-destabilizing cockle. We speculate that the eelgrass root-rhizome network might physically restrict cockle bioturbation to some extent (González-Ortiz et al. 2014) and that sediment resuspension by cockles might play an overall lesser role for net sediment loss in the presence of eelgrass due to particle trapping by the leaf canopy (Hendriks et al. 2008). Our results show the importance of considering such nonadditive effects, as they are difficult to extrapolate from single-species to multi-species assemblages and vice versa (Passarelli et al. 2014). Understanding threshold densities between stabilizing and destabilizing ecosystem engineers (Suchanek 1983; Hughes 1999; Volkenborn et al. 2009) is of particular importance in seagrass meadows, which are dependent on multiple feedback mechanisms that are susceptible to regime shifts and can prevent re-establishment (van der Heide et al. 2007; Maxwell et al. 2017).

#### Implications for management and restoration

Future climate scenarios predict increased wave intensities in the North Atlantic (Collins et al. 2019), with consequences for sediment dynamics in coastal environments (Ranasinghe 2016). In the Baltic Sea, higher significant wave heights are predicted (Groll et al. 2017) and alterations to shoreline dynamics are already detectable (Orviku et al. 2003). Although the erosion rates we measured here may not be completely comparable to field conditions at similar shear velocities, due to the short compaction time and thus limited biofilm establishment (Yallop et al. 1994), our study provides a mechanistic insight in sedimentary processes of coastal environments under the presence of co-occurring ecosystem engineers. Our results support the relevance of eelgrass meadows for coastal sediment stabilization (Ondiviela et al. 2014), and further underpin the importance of positive interactions with associated synergistic ecosystem engineers (e.g., *L. balthica*). In areas where tidal currents dominate as hydrodynamic force over waves, however, the additive positive effect of infaunal bivalves might be limited, as here resuspension plays a critical role for sediment transport and might be enhanced through bioturbation (Willows et al. 1998; Ciutat et al. 2007).

As eelgrass meadows are in decline in many parts of the world (Waycott et al. 2009), significant efforts are needed to guide restoration and conservation. Uprooting of transplanted shoots through wave disturbance is a common bottleneck for seagrass restoration (van Katwijk et al. 2016). In our experiments, shoot dislodgement was negligible ( $< 1.5\%$ ) at low wave exposures, but increased to 10–45% at higher wave exposure ( $\geq 20 \text{ cm s}^{-1}$ ). Anchoring techniques, such as hessian bags (Unsworth et al. 2019), artificial structures that mimic eelgrass below-ground structure (Temminck et al. 2020; van der Heide et al. 2021), or co-restoration with facilitative species (Gagnon et al. 2020; Reeves et al. 2020) may be necessary for successful restoration in exposed environments. Although interactions between eelgrass and *L. balthica* are likely context dependent (Meysick et al. 2020), our results indicate that co-restoration in sandy, wave-exposed sites may not only contribute to sediment stabilization, but also result in positive feedbacks for patch establishment through mutual anchoring, leading to faster recovery of essential eelgrass meadows.

#### References

- Angelini, C., T. van der Heide, J. N. Griffin, J. P. Morton, M. Derksen-Hooijberg, L. P. Lamers, A. J. Smolders, and B. R. Silliman. 2015. Foundation species' overlap enhances biodiversity and multifunctionality from the patch to landscape scale in southeastern United States salt marshes. *Proc. Natl. Acad. Sci. USA* **282**: 20150421. doi:10.1098/rspb.2015.0421
- Angelini, C., J. N. Griffin, J. van de Koppel, L. P. M. Lamers, A. J. P. Smolders, M. Derksen-Hooijberg, T. van der Heide, and B. R. Silliman. 2016. A keystone mutualism underpins

- resilience of a coastal ecosystem to drought. *Nat. Commun.* **7**: 8–16. doi:10.1038/ncomms12473
- Boström, C., and E. Bonsdorff. 1997. Community structure and spatial variation of benthic invertebrates associated with *Zostera marina* (L.) beds in the northern Baltic Sea. *J. Sea Res.* **37**: 153–166. doi:10.1016/S1385-1101(96)00007-X
- Boström, C., and others. 2014. Distribution, structure and function of Nordic eelgrass (*Zostera marina*) ecosystems: implications for coastal management and conservation. *Aquat. Conserv. Mar. Freshwat. Ecosyst.* **24**: 410–434. doi:10.1002/aqc.2424
- Bouma, T. J., S. Olenin, K. Reise, and T. Ysebaert. 2009. Ecosystem engineering and biodiversity in coastal sediments: posing hypotheses. *Helgol. Mar. Res.* **63**: 95–106. doi:10.1007/s10152-009-0146-y
- Bouma, T. J., and others. 2014. Identifying knowledge gaps hampering application of intertidal habitats in coastal protection: Opportunities & steps to take. *Coast. Eng.* **87**: 147–157. doi:10.1016/j.coastaleng.2013.11.014
- Chen, S., L. P. Sanford, E. W. Koch, F. Shi, and E. W. North. 2007. A nearshore model to investigate the effects of seagrass bed geometry on wave attenuation and suspended sediment transport. *Estuar. Coast.* **30**: 296–310. doi:10.1007/BF02700172
- Ciutat, A., J. Widdows, and N. D. Pope. 2007. Effect of *Cerastoderma edule* density on near-bed hydrodynamics and stability of cohesive muddy sediments. *J. Exp. Mar. Biol. Ecol.* **346**: 114–126. doi:10.1016/j.jembe.2007.03.005
- Collins, M., and others. 2019. Extremes, abrupt changes and managing risk. In H. O. Pörtner and others [eds.], IPCC special report on the ocean and cryosphere in a changing climate. <https://www.ipcc.ch/srocc/chapter/chapter-6/>
- Cozzoli, F., and others. 2020. Biological and physical drivers of bio-mediated sediment resuspension: A flume study on *Cerastoderma edule*. *Estuar. Coast. Shelf Sci.* **241**: 106824. doi:10.1016/j.ecss.2020.106824
- Damveld, J. H., and others. 2018. Video transects reveal that tidal sand waves affect the spatial distribution of benthic organisms and sand ripples. *Geophys. Res. Lett.* **45**: 11837–11846. doi:10.1029/2018GL079858
- Danovaro, R., M. Armeni, A. Dell'Anno, M. Fabiano, E. Manini, D. Marrale, A. Pusceddu, and S. Vanucci. 2001. Small-scale distribution of bacteria, enzymatic activities, and organic matter in coastal sediments. *Microb. Ecol.* **42**: 177–185. doi:10.1007/s002480000109
- de Paiva, J. N. S., B. Walles, T. Ysebaert, and T. J. Bouma. 2018. Understanding the conditionality of ecosystem services: The effect of tidal flat morphology and oyster reef characteristics on sediment stabilization by oyster reefs. *Ecol. Eng.* **112**: 89–95.
- Donadi, S., and others. 2014. The bivalve loop: Intra-specific facilitation in burrowing cockles through habitat modification. *J. Exp. Mar. Biol. Ecol.* **461**: 44–52. doi:10.1016/j.jembe.2014.07.019
- Donadi, S., and others. 2015. Multi-scale habitat modification by coexisting ecosystem engineers drives spatial separation of macrobenthic functional groups. *Oikos* **124**: 1502–1510. doi:10.1111/oik.02100
- Dugge, J. (2022). Calculate DEM surface area. MATLAB Central File Exchange [accessed 2021 March 12]. Available from <https://www.mathworks.com/matlabcentral/fileexchange/42204-calculate-dem-surface-area>.
- Fales, R. J., F. C. Boardman, and J. L. Ruesink. 2020. Reciprocal interactions between bivalve molluscs and seagrass: A review and meta-analysis. *J. Shellfish Res.* **39**: 547–562. doi:10.2983/035.039.0305
- Flynn, P. T., K. McCarvill, K. D. Lynn, and P. A. Quijón. 2020. The positive effect of coexisting ecosystem engineers: A unique seaweed-mussel association provides refuge for native mud crabs against a non-indigenous predator. *PeerJ.* **8**: e10540. doi:10.7717/peerj.10540
- Fonseca, M. S., J. S. Fisher, J. C. Zieman, and G. W. Thayer. 1982. Influence of the seagrass, *Zostera marina* L., on current flow. *Estuar. Coast. Shelf Sci.* **15**: 351–364. doi:10.1016/0272-7714(82)90046-4
- Gagnon, K., and others. 2020. Facilitating foundation species: The potential for plant–bivalve interactions to improve habitat restoration success. *J. Appl. Ecol.* **57**: 1161–1179. doi:10.1111/1365-2664.13605
- Garzon, J. L., M. Maza, C. M. Ferreira, J. L. Lara, and I. J. Losada. 2019. Wave attenuation by *Spartina* saltmarshes in the Chesapeake Bay under storm surge conditions. *J. Geophys. Res. Oceans* **124**: 5220–5243. doi:10.1029/2018JC014865
- González-Ortiz, V., P. Alcazar, J. J. Vergara, J. L. Pérez-Lloréns, and F. G. Brun. 2014. Effects of two antagonistic ecosystem engineers on infaunal diversity. *Estuarine, Coast. Shelf Sci.* **139**: 20–26. doi:10.1016/j.ecss.2013.12.015
- Gregow, H., A. Laaksonen, and M. E. Alper. 2017. Increasing large scale windstorm damage in Western, Central and Northern European forests, 1951–2010. *Sci. Rep.* **7**: 46397. doi:10.1038/srep46397
- Groll, N., I. Grabemann, B. Hünicke, and M. Meese. 2017. Baltic Sea wave conditions under climate change scenarios. *Boreal Environ. Res.* **22**: 1–12.
- Gutiérrez, J. L., and others. 2011. Physical ecosystem engineers and the functioning of estuaries and coasts, p. 53–81. In E. Wolanski and D. S. McClusky [eds.], *Treatise on estuarine and coastal science*. Academic Press.
- Halpern, B. S., and others. 2008. A global map of human impact on marine ecosystems. *Science* **319**: 948–952. doi:10.1126/science.1149345
- Hansen, J. C., and M. A. Reidenbach. 2012. Wave and tidally driven flows in eelgrass beds and their effect on sediment suspension. *Mar. Ecol. Prog. Ser.* **448**: 271–287. doi:10.3354/meps09225

- Hendriks, I. E., T. Sintes, T. J. Bouma, and C. M. Duarte. 2008. Experimental assessment and modeling evaluation of the effects of the seagrass *Posidonia oceanica* on flow and particle trapping. *Mar. Ecol. Prog. Ser.* **356**: 163–173. doi:10.3354/meps07316
- Herkül, K., and J. Kotta. 2009. Effects of eelgrass (*Zostera marina*) canopy removal and sediment addition on sediment characteristics and benthic communities in the Northern Baltic Sea. *Mar. Ecol. Prog. Ser.* **30**: 74–82. doi:10.1111/j.1439-0485.2009.00307.x
- Hughes, R. G. 1999. Saltmarsh erosion and management of saltmarsh restoration; the effects of infaunal invertebrates. *Aquat. Conserv. Mar. Freshwat. Ecosyst.* **9**: 83–95 doi:10.1002/(SICI)1099-0755(199901/02)9:1<83::AID-AQC323>3.0.CO;2-9.
- Huxham, M., and others. 2010. Intra- and interspecific facilitation in mangroves may increase resilience to climate change threats. *Philos. Trans. R. Soc. B.* **365**: 2127–2135. doi:10.1098/rstb.2010.0094
- Infantes, E., A. Orfila, G. Simarro, J. Terrados, M. Luhar, and H. Nepf. 2012. Effect of a seagrass (*Posidonia oceanica*) meadow on wave propagation. *Mar. Ecol. Prog. Ser.* **456**: 63–72. doi:10.3354/meps09754
- Infantes, E., J. de Smit, E. Tamarit, and T. J. Bouma. 2021. Making realistic wave climates in low-cost wave mesocosms: A new tool for experimental ecology and biogeomorphology. *Limnol. Oceanogr. Methods* **19**: 317–330. doi:10.1002/lom3.10425
- Jones, C. G., J. H. Lawton, and M. Shachak. 1994. Organisms as ecosystem engineers. *Oikos* **69**: 373–386. doi:10.2307/3545850
- Jönsson, A., Å. Danielsson, and L. Rahm. 2005. Bottom type distribution based on wave friction velocity in the Baltic Sea. *Cont. Shelf Res.* **25**: 419–435.
- Łabuz, T. A. 2015. Environmental impacts—coastal erosion and coastline changes, p. 381–396. *In* The BACC II Author Team [ed.], Second assessment of climate change for the Baltic Sea basin. Springer.
- Leon, J. X., C. M. Roelfsema, M. I. Saunders, and S. R. Phinn. 2015. Measuring coral reef terrain roughness using “Structure-from-Motion” close-range photogrammetry. *Geomorphology* **242**: 21–28. doi:10.1016/j.geomorph.2015.01.030
- Lindgarth, M., C. André, and P. R. Jonsson. 1995. Analysis of the spatial variability in abundance and age structure of two infaunal bivalves, *Cerastoderma edule* and *C. lamarcki*, using hierarchical sampling programs. *Mar. Ecol. Prog. Ser.* **116**: 85–97.
- Luhar, M., E. Infantes, and H. Nepf. 2017. Seagrass blade motion under waves and its impact on wave decay. *J. Geophys. Res. Ocean.* **122**: 3736–3752.
- Mallison, H., and O. Wings. 2014. Photogrammetry in paleontology—A practical guide. *JPT.* **12**: 1–31.
- Marin-Diaz, B., T. J. Bouma, and E. Infantes. 2020. Role of eelgrass on bedload transport and sediment resuspension under oscillatory flow. *Limnol. Oceanogr.* **65**: 426–436. doi:10.1002/lno.11312
- Maxwell, P. S., and others. 2017. The fundamental role of ecological feedback mechanisms for the adaptive management of seagrass ecosystems—A review. *Biol. Rev.* **92**: 1521–1538. doi:10.1111/brv.12294
- Meadows, P. S., A. Meadows, F. J. West, P. S. Shand, and M. A. Shaikh. 1998. Mussels and mussel beds (*Mytilus edulis*) as stabilizers of sedimentary environments in the intertidal zone. *Spec. Publ. Geol. Soc. Lond.* **139**: 331–347. doi:10.1144/GSL.SP.1998.139.01.26
- Meysick, L., E. Infantes, and C. Boström. 2019a. The influence of hydrodynamics and ecosystem engineers on eelgrass seed trapping. *PLoS one.* **14**: e0222020. doi:10.1371/journal.pone.0222020
- Meysick, L., T. Ysebaert, A. Jansson, F. Montserrat, S. Valanko, A. Villnäs, C. Boström, J. Norkko, and A. Norkko. 2019b. Context-dependent community facilitation in seagrass meadows along a hydrodynamic stress gradient. *J. Sea Res.* **150**: 8–23. doi:10.1016/j.seares.2019.05.001
- Meysick, L., A. Norkko, K. Gagnon, M. Gräfnings, and C. Boström. 2020. Context-dependency of eelgrass–clam interactions: Implications for coastal restoration. *Mar. Ecol. Prog. Ser.* **647**: 93–108. doi:10.3354/meps13408
- Obolewski, K., M. Konkel, A. Strzelczak, and Z. Piesik. 2007. Distribution and the role of *Cerastoderma glaucum* (Poiret, 1789) in the Polish Baltic Sea coast. *Balt. Coast. Zone* **11**: 13–24.
- Ondiviela, B., I. J. Losada, J. L. Lara, M. Maza, C. Galván, T. J. Bouma, and J. van Belzen. 2014. The role of seagrasses in coastal protection in a changing climate. *Coast. Eng.* **87**: 158–168. doi:10.1016/j.coastaleng.2013.11.005
- Orviku, K., J. Jaagus, A. Kont, U. Ratas, and R. Rivis. 2003. Increasing activity of coastal processes associated with climate change in Estonia. *J. Coast. Res.* **19**: 364–375.
- Papanicolaou, A. N., P. Diplas, C. L. Dancy, and M. Balakrishnan. 2001. Surface roughness effects in near-bed turbulence: Implications to sediment entrainment. *J. Eng. Mech.* **127**: 211–218. doi:10.1061/(ASCE)0733-9399(2001)127:3(211)
- Passarelli, C., F. Olivier, D. M. Paterson, T. Mezziane, and C. Hubas. 2014. Organisms as cooperative ecosystem engineers in intertidal flats. *J. Sea Res.* **92**: 92–101. doi:10.1016/j.seares.2013.07.010
- R Core Team (2017). R: A language and environment for statistical computing. R Foundation for Statistical Computing. Available from <https://www.R-project.org/>.
- Ranasinghe, R. 2016. Assessing climate change impacts on open sandy coasts: A review. *Earth-Sci. Rev.* **160**: 320–332. doi:10.1016/j.earscirev.2016.07.011
- Reeves, S. E., J. J. Renzi, E. K. Fobert, B. R. Silliman, B. Hancock, and C. L. Gillies. 2020. Facilitating better outcomes: How positive species interactions can improve



- oyster reef restoration. *Front. Mar. Sci.* **7**: 656. doi:[10.3389/fmars.2020.00656](https://doi.org/10.3389/fmars.2020.00656)
- Reusch, T. B., and A. R. Chapman. 1995. Storm effects on eelgrass (*Zostera marina* L.) and blue mussel (*Mytilus edulis* L.) beds. *J. Exp. Mar. Biol. Ecol.* **192**: 257–271. doi:[10.1016/0022-0981\(95\)00074-2](https://doi.org/10.1016/0022-0981(95)00074-2)
- Roebeling, P. C., L. Costa, L. Magalhães-Filho, and V. Tekken. 2013. Ecosystem service value losses from coastal erosion in Europe: historical trends and future projections. *J. Coast. Conserv.* **17**: 389–395. doi:[10.1007/s11852-013-0235-6](https://doi.org/10.1007/s11852-013-0235-6)
- Shepard, M. K., and others. 2001. The roughness of natural terrain: A planetary and remote sensing perspective. *J. Geophys. Res. Planets*, **106**(E12): 32777–32795. doi:[10.1029/2000JE001429](https://doi.org/10.1029/2000JE001429)
- Suchanek, T. H. 1983. Control of seagrass communities and sediment distribution by *Callianassa* (Crustacea, Thalassinidea) bioturbation. *J. Mar. Res.* **41**: 281–298. doi:[10.1357/002224083788520216](https://doi.org/10.1357/002224083788520216)
- Temmink, R. J., and others. 2020. Mimicry of emergent traits amplifies coastal restoration success. *Nat. Commun.* **11**: 1–9. doi:[10.1038/s41467-020-17438-4](https://doi.org/10.1038/s41467-020-17438-4)
- Unsworth, R. K., C. Bertelli, L. Cullen-Unsworth, N. Esteban, R. Lilley, B. L. Jones, C. Lowe, H. Nuuttila, and S. Rees. 2019. Sowing the seeds of seagrass recovery using hessian bags. *Front. Ecol. Evol.* **7**: 311. doi:[10.3389/fevo.2019.00311](https://doi.org/10.3389/fevo.2019.00311)
- van der Heide, T., E. H. van Nes, G. W. Geerling, A. J. Smolders, T. J. Bouma, and M. M. van Katwijk. 2007. Positive feedbacks in seagrass ecosystems: implications for success in conservation and restoration. *Ecosystems* **10**: 1311–1322. doi:[10.1007/s10021-007-9099-7](https://doi.org/10.1007/s10021-007-9099-7)
- van der Heide, T., and others. 2021. Coastal restoration success via emergent trait-mimicry is context dependent. *Biol. Conserv.* **264**: 109373. doi:[10.1016/j.biocon.2021.109373](https://doi.org/10.1016/j.biocon.2021.109373)
- van Katwijk, M. M., and others. 2016. Global analysis of seagrass restoration: the importance of large-scale planting. *J. Appl. Ecol.* **53**: 567–578. doi:[10.1111/1365-2664.12562](https://doi.org/10.1111/1365-2664.12562)
- Volkenborn, N., D. M. Robertson, and K. Reise. 2009. Sediment destabilizing and stabilizing bio-engineers on tidal flats: Cascading effects of experimental exclusion. *Helgol. Mar. Res.* **63**: 27–35. doi:[10.1007/s10152-008-0140-9](https://doi.org/10.1007/s10152-008-0140-9)
- Waycott, M., and others. 2009. Accelerating loss of seagrasses across the globe threatens coastal ecosystems. *Proc. Natl. Acad. Sci. USA* **106**: 12377–12381. doi:[10.1073/pnas.0905620106](https://doi.org/10.1073/pnas.0905620106)
- Wiberg, P. L., S. R. Taube, A. E. Ferguson, M. R. Kremer, and M. A. Reidenbach. 2019. Wave attenuation by oyster reefs in shallow coastal bays. *Estuar. Coast.* **42**: 331–347. doi:[10.1007/s12237-018-0463-y](https://doi.org/10.1007/s12237-018-0463-y)
- Widdows, J., N. D. Pope, M. D. Brinsley, H. Asmus, and R. M. Asmus. 2008. Effects of seagrass beds (*Zostera noltii* and *Z. marina*) on near-bed hydrodynamics and sediment resuspension. *Mar. Ecol. Prog. Ser.* **358**: 125–136. doi:[10.3354/meps07338](https://doi.org/10.3354/meps07338)
- Willows, R. I., J. Widdows, and R. G. Wood. 1998. Influence of an infaunal bivalve on the erosion of an intertidal cohesive sediment: a flume and modeling study. *Limnol. Oceanogr.* **43**: 1332–1343. doi:[10.4319/lo.1998.43.6.1332](https://doi.org/10.4319/lo.1998.43.6.1332)
- Yallop, M. L., B. de Winder, D. M. Paterson, and L. J. Stal. 1994. Comparative structure, primary production and biogenic stabilization of cohesive and non-cohesive marine sediments inhabited by microphytobenthos. *Estuar. Coast. Shelf Sci.* **39**: 565–582.
- Ysebaert, T., B. Walles, J. Haner, and B. Hancock. 2019. Habitat modification and coastal protection by ecosystem-engineering reef-building bivalves, p. 253–273. *In* A. C. Smaal, J. G. Ferreira, J. Grant, J. K. Petersen, and Ø. Strand [eds.], *Goods and services of marine bivalves*. Springer.
- Ziebis, W., M. Huettel, and S. Forster. 1996. Impact of biogenic sediment topography on oxygen fluxes in permeable seabeds. *Mar. Ecol. Prog. Ser.* **140**: 227–237. doi:[10.3354/meps140227](https://doi.org/10.3354/meps140227)

#### Acknowledgments

This project received funding from the European Union's Horizon 2020 research and innovation program as part of the project MERCES: Marine Ecosystem Restoration in Changing European Seas (grant agreement no. 689518). Travel and experiments at Kristineberg were funded by the Royal Swedish Academy of Science (KVA). L.M. further received funding from the Functional Marine Biodiversity Network (FunMarBio) at Åbo Akademi University. C.B. was funded through the Åbo Akademi University Foundation Sr. E.I received funds from FORMAS Dnr. 2019-01192. The wave mesocosms at the Archipelago Centre Korpoström were custom made at the Royal Netherlands Institute for Sea Research (NIOZ-Yerseke) and these research infrastructure facilities were provided by FINMARI (Finnish Marine Research Infrastructure network). Albert Boström is acknowledged for field assistance in Kristineberg. The authors would also like to thank two anonymous reviewers and the Associate editor for helpful comments to improve this manuscript. Open Access funding enabled and organized by Projekt DEAL.

#### Conflict of Interest

None declared.

Submitted 22 March 2021

Revised 23 September 2021

Accepted 07 January 2022

Associate editor: Josef Daniel Ackerman